JACC: CARDIOVASCULAR IMAGING
VOL. 7, NO. 7, 2014

ISSN 1936-878X/$36.00
PUBLISHED BY ELSEVIER INC.
http://dx.doi.org/10.1016/j.jcmg.2014.01.014

CMR-Guided Approach to Localize and Ablate Gaps in Repeat AF Ablation Procedure

Felipe Bisbal, MD, Esther Guiu, MSc, Pilar Cabanas-Grandío, MD, Antonio Berruezo, MD, PhD, Susana Prat-Gonzalez, MD, PhD, Bárbara Vidal, MD, PhD, Cesar Garrido, RT, David Andreu, MSc, PhD, Juan Fernandez-Armenta, MD, Jose María Tolosana, MD, Elena Arbelo, MD, PhD, Teresa M. de Caralt, MD, PhD, Rosario J. Perea, MD, PhD, Josep Brugada, MD, PhD, Lluís Mont, MD, PhD

ABSTRACT

OBJECTIVES The aim of this study was to test the feasibility and usefulness of a new delayed-enhancement cardiac magnetic resonance (DE-CMR)–guided approach to ablate gaps in redo procedures.

BACKGROUND Recurrences of atrial fibrillation (AF) after pulmonary vein isolation (PVI) may be related to gaps at the ablation lines. DE-CMR allows identification of radiofrequency lesions and gaps (CMR gaps).

METHODS Fifteen patients undergoing repeated AF ablations were included (prior procedure was PVI in all patients and roof-line ablation in 8 patients). Pre-procedure 3-dimensional (3D) DE-CMR was performed with a respiratory-navigated (free-breathing) and electrocardiographically gated inversion-recovery gradient-echo sequence (voxel size 1.25 × 1.25 × 2.5 mm). Endocardium and epicardium were manually segmented to create a 3D reconstruction (DE-CMR model). A pixel signal intensity map was projected on the DE-CMR model and color-coded (thresholds 40 ± 5% and 60 ± 5% of maximum intensity). The DE-CMR model was imported into the navigation system to guide the ablation of CMR gaps, with the operator blinded to electrical data. Fifteen conventional procedures were used as controls to compare procedural duration, radiofrequency, and fluoroscopy times.

RESULTS Fifteen patients (56 pulmonary veins [PVs]; 57 ± 8 years of age; 9 with paroxysmal AF) were analyzed. In total, 67 CMR gaps were identified around PVs (mean 4.47 gaps/patient; median length 13.33 mm/gap) and 9 at roof line. All of the electrically reconnected PVs (87.5%) had CMR gaps. The site of electrical PV reconnection (assessed by circular mapping catheter) matched with a CMR gap in 79% of PVs. CMR-guided ablation led to reisolation of 95.6% of reconnected PVs (median radiofrequency time of 13.3 [interquartile range: 7.5 to 21.7] min/patient) and conduction block through the roof line in all patients (1.4 [interquartile range: 0.7 to 3.1] min/patient). Compared with controls, the CMR-guided approach shortened radiofrequency time (1,441 ± 915 s vs. 930 ± 662 s; $p = 0.026$) but not the procedural duration or fluoroscopy time.

CONCLUSIONS DE-CMR can successfully guide repeated PVI procedures by accurately identifying and localizing gaps and may reduce procedural duration and radiofrequency application time. (J Am Coll Cardiol Img 2014;7:653–63) © 2014 by the American College of Cardiology Foundation.

Pulmonary vein isolation (PVI) has become a first-line treatment for symptomatic drug-refractory atrial fibrillation (AF), although short- and mid-term success remains only moderate (1–3). More recently, substrate modification targeting complex fractionated electrograms and deployment

From the Unitat de Fibrilació Auricular, Hospital Clínic, Institut d'Investigacions Biomèdiques August Pi i Sunyer, Barcelona, Catalonia, Spain. This study was supported by Instituto de Salud Carlos III, Ministerio de Economía y Competitividad, Spain (PI11/02049, PI1102003, REDSINCOR RD06/0003/008, and Red HERACLES RD06/0009) and by Fondo Europeo de Desarrollo Regional, European Union. Dr. Cabanas was supported by a grant of Sección de Arritmias y Electrofisiología (Sociedad Española de Cardiología). Dr. Andreu is employed by Biosense Webster. Dr. Mont has served as a consultant for Biosense Webster, Boston Scientific, and St. Jude Medical. All other authors have reported that they have no relationships relevant to the contents of this paper to disclose.

Manuscript received November 4, 2013; revised manuscript received December 16, 2013, accepted January 10, 2014.

ABBREVIATIONS AND ACRONYMS

AF = atrial fibrillation

DE-CMR = delayed-enhancement cardiac magnetic resonance

LA = left atrium

PVI = pulmonary vein isolation

RF = radiofrequency

SI = signal intensity

of additional ablation lines have been implemented to improve outcomes, mostly in patients with persistent AF. Despite increasing experience and progress in ablation techniques, a large proportion of patients still require repeat procedures for AF or for organized macroreentrant tachycardia. Pulmonary vein (PV) reconnection is considered the main cause for procedural failure (4,5), and discontinuities in previous ablation sets are a common underlying mechanism for resumption of conduction (6,7).

SEE PAGE 664

Delayed-enhancement cardiac magnetic resonance (DE-CMR) allows the identification of radiofrequency (RF) lesions in the myocardium (8). Peters et al. (9) first identified RF-related scarring with this image modality in the PVI setting; several studies have confirmed its use (10,11), although its reproducibility has been questioned (12). A recent experimental study in a swine model showed how real-time DE-CMR can depict gaps in acute ablation lesion sets and guide the ablation (13). Studies are now needed to evaluate the usefulness of direct DE-CMR guidance during the ablation procedure in humans. The present study describes the initial experience using a DE-CMR approach to localize gaps in previous ablation lesions and guide repeated ablation procedures in humans.

METHODS

STUDY POPULATION. Fifteen consecutive eligible patients with atrial arrhythmia recurrence after PVI and indication for repeat procedure were prospectively enrolled between June 2012 and March 2013. The study protocol was approved by the hospital's ethics committee. The inclusion criteria were: 1) drug-refractory AF or atypical atrial flutter after a first percutaneous PVI procedure (excluding a 3-month blanking period); and 2) written informed consent. The exclusion criteria included: 1) age <18 years; and 2) contraindication for a 3-T cardiac magnetic resonance (CMR) (advanced renal failure, morbid obesity, pacemaker/implantable cardioverter-defibrillator, prior adverse events to magnetic contrast agent, or pregnancy).

A series of 15 consecutive clinically matched patients of the same operators who underwent a second conventional Lasso-technique PVI were the control group to compare procedural duration and RF and fluoroscopy time.

IMAGE POST-PROCESSING. A detailed description of the DE-CMR acquisition protocol is provided in the Online Appendix. All DE-CMR images were analyzed with self-customized software (Tissue Characterization Tool Kit) based on MATLAB (The MathWorks, Natick, Massachusetts), as previously described (14). Masked to clinical information, an experienced observer manually traced epicardium and endocardium borders on axial-plane slices. Full LA volume was reconstructed in the axial orientation, and the resulting images were processed with GIMIAS (15,16). Five concentric surface layers without thickness were created automatically, from endocardium to epicardium, at 10%, 25%, 50%, 75%, and 90% of LA wall thickness, respectively. A 3-dimensional (3D) shell was obtained for each layer, but only 1 shell was selected for the reablation procedure and data analysis. We selected the shell that was entirely within the LA wall (usually 25% or 50%), which ensured that extracardiac structures as pericardium, blood pool, or descending aorta were not picked up. Pixel signal intensity (SI) maps obtained from DE-CMR were projected to each shell and color-coded. Each of the shells contained on average 60,000 triangles (mean edge length of 0.45 mm). The value of the SI of each triangle was obtained from a sum of different coefficients; the main coefficient was obtained from the SI of the voxel and the other from the SI of the surrounding voxels weighted by the distance to the triangle. For identification of the prior ablation lesions and gaps, a pixel SI-based algorithm was applied to characterize the hyperenhanced area as scar core or border zone, using 40 ± 5% and 60 ± 5% of the maximum intensity as thresholds (14,17). The resulting processed images of the selected shell were used to create a DE-CMR model that was integrated into the CARTO 3 system (Biosense Webster, Diamond Bar, California) to guide the ablation procedure (**Fig. 1**).

A CMR gap was defined as any discontinuity of previous ablation lesions (scar core) and was quantified as gap length (in mm). Border zone was not taken into account for gap definition.

REABLATION PROCEDURE. A detailed description of the prior ablation procedure is provided in the Online Appendix. Previously described institutional standard protocols of sedation and anticoagulation were applied (18). Electrical cardioversion was performed if AF was present at the time of reablation.

High-density voltage mapping was performed using the CARTO 3 system and a 3.5-mm, open-irrigation tip, contact-force catheter (Smart-Touch, Biosense Webster). To avoid false low-voltage sites, points were acquired only for contact force above

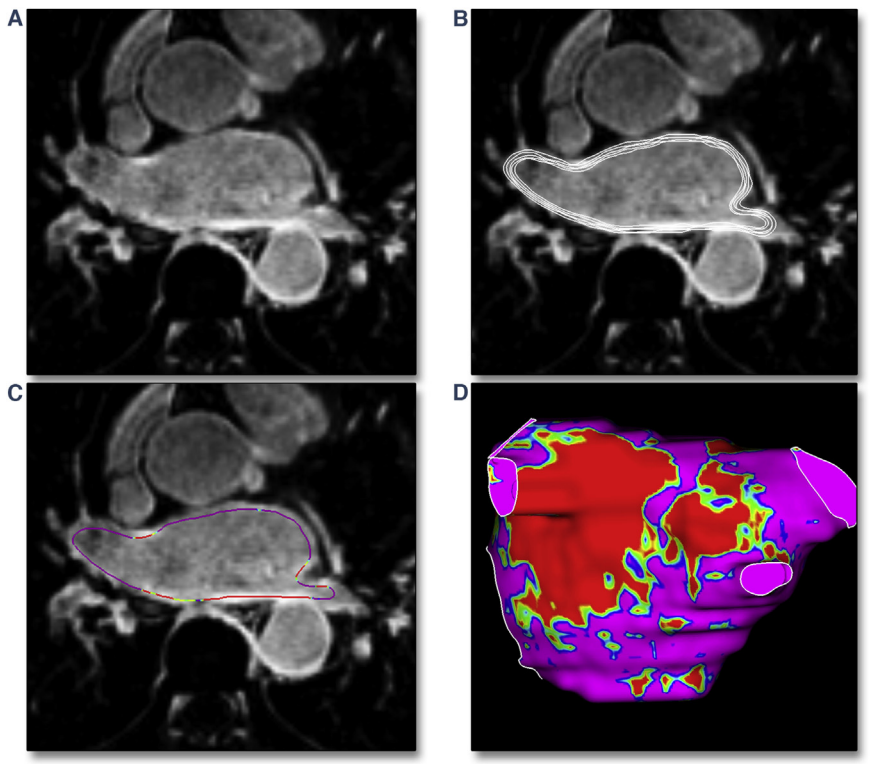

FIGURE 1 Image Post-Processing

(A) Axial plane of a delayed-enhancement cardiac magnetic resonance (DE-CMR) imaging scan at the atrial level. **(B)** After manual segmentation of endocardium and epicardium, 5 concentric surface layers were created at 10%, 25%, 50%, 75%, and 90% ("onion skin" model). **(C)** Pixel intensity map was projected and **(D)** 3-dimensional shell obtained for each layer. In this patient, a left atrial flutter was documented after the first atrial fibrillation ablation. The DE-CMR model identified a possible anatomic isthmus at the posterior wall between the 2 scarred areas related to prior circumferential ablation lesions. After pulmonary vein reisolation, a single radiofrequency application between prior circumferential lesions at the posterior wall led to bidirectional block. A burst pacing protocol did not trigger any atrial arrhythmia.

10 g. Color-coded DE-CMR LA reconstruction was integrated into the navigation system using at least 4 pre-defined PV ostia sites as landmark points and surface registration. A circular multipolar catheter (Lasso, Biosense Webster) was introduced to localize the PV reconnection sites, identified as the earliest PV electrogram in the activation sequence at the PV antrum. A second operator ablated the CMR gaps, blinded to circular mapping catheter and voltage mapping information and guided only by the color-coded DE-CMR model. For each PV, ablation stopped when isolation was achieved. PVI was checked as described earlier.

Post-ablation management was performed as described elsewhere (3).

COMPARISON BETWEEN ELECTROPHYSIOLOGICAL AND DE-CMR DATA. The signal amplitude (mV) of the CARTO map was evaluated for the different tissue categories of the DE-CMR model (scar, border zone, and healthy myocardium). For this purpose, the points of the electroanatomic map were co-registered with the DE-CMR model, and the mean (SD) voltage was calculated for each of the 3 tissue categories.

Electrophysiological data was compared with DE-CMR findings to assess the accuracy of the imaging technique in predicting PV reconnection and in identifying the site of PV reconnection, as well as to compare the capability of both techniques in depicting the ablation lesions and gaps.

- Electrogram-CMR concordance evaluates the capability of the DE-CMR to predict electrical PV reconnection and was defined per each PV as presence of CMR gaps with electrical reconnection or absence of CMR gaps with PVI.
- The reconnection sites were assessed by the circular multipolar catheter and compared with CMR.

Agreement between techniques was considered when the earliest activation site in the Lasso catheter matched a CMR gap.

- Comparison between voltage map and DE-CMR to evaluate the accuracy to define anatomic gaps of both techniques (voltage vs. CMR gaps). Agreement between both techniques was considered to be present when a voltage gap concurred with a CMR gap.

STATISTICAL ANALYSIS. Continuous data are expressed as mean ± SD, median, or interquartile range (IQR) as appropriate. Nominal data are expressed as n (%). The chi-square or Fisher exact test was used to compare proportions between the groups, and Student *t*, paired *t*, Friedman, or Mann-Whitney *U* test was used for continuous variables as appropriate. A p value ≤0.05 was considered significant. Statistical analyses were performed using SPSS 18.0 (SPSS, Chicago, Illinois).

RESULTS

PATIENT POPULATION. This prospective study included 15 consecutive unselected patients with AF recurrence after prior PVI procedure (12 men; mean age 57 ± 8 years; 9 [60%] with paroxysmal AF; median time from prior PVI 15 months [IQR: 9 to 22 months]) (Online Fig. 1). Baseline patient characteristics are summarized in **Table 1**. Before CMR, 2 patients underwent electrical cardioversion due to AF. The median time from CMR to the ablation procedure was 7 (IQR: 1 to 16 days) days. After a mean follow-up of 8.5 ± 4.1 months, 3 patients (20%) had AF recurrence beyond the blanking period.

DE-CMR GAP CHARACTERISTICS. In total, 56 PVs were identified. A left common trunk was found in 4 patients; the remaining 11 patients had 4 independent PV ostia (**Table 2**). The gap characterization analysis was performed in 53 PVs (3 PVs were excluded from this analysis due to the complete absence of scarring). Sixty-seven CMR gaps were identified around the PVs (mean of 4.47 gaps/patient and 1.27 ± 0.41 gaps/PV). The right superior PV showed the highest number of gaps (mean of 1.53 gaps) and the left inferior pulmonary vein (LIPV) the fewest (mean of 0.67 gaps). The median gap length was 13.33 ± 5.8 mm/gap (minimum of 1.6 mm). The majority of patients (73.3%) had CMR gaps in all PVs.

PV RECONNECTION. In total, 49 PVs were electrically reconnected; all of them showing CMR gaps (46 PVs) or complete absence of scarring (3 PVs). The remaining 7 PVs were electrically isolated; 3 of them showed CMR gaps and 4 had complete encircling lesions (Online Fig. 2). The electrogram-CMR concordance was 94.6% (53 of 56 PV). The presence of CMR gaps in electrically isolated PVs precluded concordance in 3 PVs (5.4%) (**Table 2**).

The site of electrical PV reconnection was assessed in the PVs in which the position of the circular mapping catheter was strictly perpendicular to the PV

TABLE 1 Baseline and Prior Procedure Characteristics of Included Patients

Patient #	Age, yrs	Sex	HT	DM	CHA_2DS_2-VASc	LAD	AF Type	AAD	Ablation Technique	Time to Recurrence, months	Time to Second Procedure, months
1	55	M	No	No	0	44	Px	A, B	PVI, RL	1	9
2	60	M	Yes	No	1	43	Pr	Fl, B	PVI, RL, CFAE	11	21
3	71	F	Yes	No	3	53	Px	A	PVI, RL, PL	20	28
4	63	M	Yes	Yes	2	46	Px	A	PVI	3	14
5	56	M	Yes	Yes	2	43	Pr	A, B	PVI, ML	4	22
6	65	F	No	No	1	37	Pr	Fl	PVI	6	15
7	49	M	Yes	No	1	42	Pr	Fl, B	PVI, RL, PL	9	95
8	50	M	No	No	0	50	Pr	A, B	PVI, RL	13	19
9	60	F	Yes	No	2	42	Px	A	PVI	1	7
10	48	M	No	No	0	49	Px	Fl	Cryoballoon	4	9
11	72	M	No	No	1	35	Px	A	PVI, RL, PL	14	20
12	62	M	No	No	0	35	Px	Fl, B	PVI, RL	20	42
13	43	M	No	No	0	47	Pr	A	PVI, RL, CFAE	6	12
14	56	M	Yes	No	2	46	Px	A	PVI	1	3
15	45	M	No	No	0	40	Px	Fl	Cryoballoon	4	7

A = amiodarone; AAD = antiarrhythmic drugs; AF = atrial fibrillation; B = beta-blockers; CFAE = complex and fractionated atrial electrogram ablation; DM = diabetes mellitus; F = female; Fl = flecainide; HT = hypertension; LAD = left atrial diameter; M = male; ML = mitral line; PL = posterior line; Pr = persistent; PVI = pulmonary vein isolation; Px = paroxysmal; RL = roof line.

TABLE 2 Electroanatomic Mapping and DE-CMR Findings

Patient #	Total CMR-Gaps, PVs	Total PV Length, mm	Total Length per Gap, mm	% Gap Length of Total PVs Perimeter	PV With CMR Gaps	Reconnected PVs	Concordance (%)	EAM Points
All	4.47 ± 1.25	74.06 ± 9.93	13.30 ± 5.78	22.49 ± 9.98	49/53	46/53	93.8	808 (626-878)
1	4	64.75	5.85	9.03	4/4	4/4	100	586
2	5	66.75	11.68	21.87	4/4	4/4	100	633
3	4	69.75	5.95	8.53	4/4	4/4	100	719
4	6	70.50	8.20	17.45	4/4	3/4	75	626
5	5	88.33	16.52	31.17	3/3	3/3*	100	1004
6	4	93.33	9.30	13.29	3/3	2/3*	66	856
7	4	73.50	23.60	32.11	4/4	3/4	75	978
8	2	75.50	10.50	13.91	2/2	2/2	100	875
9	3	78.67	22.90	29.11	3/3	3/3*	100	584
10	5	77.00	15.00	24.35	4/4	4/4	100	520
11	6	60.25	10.92	27.18	4/4	4/4	100	680
12	6	70.33	15.80	44.93	3/3	3/3*	100	848
13	3	87.00	19.33	16.67	2/4	2/4	100	898
14	6	59.00	7.32	18.60	3/4	3/4	100	878
15	4	76.33	16.33	29.21	2/3	2/3	100	812

*Presence of a left common trunk.

DE-CMR = delayed-enhancement cardiac magnetic resonance; EAM = electroanatomic map; PV = pulmonary vein; other abbreviation as in Table 1.

ostium (18 PVs). The position of the dipole registering the earliest activation matched with a CMR gap in 79% of PVs (Fig. 2).

In 8 PVs (14.3%), PV cannulation with the circular multipolar catheter was not feasible (4 LIPVs, 2 right inferior PVs, and 2 left superior PVs [LSPVs]). In one case, PV stenosis caused the cannulation failure (LSPV of 0.6 cm). The other PVs were normal sized (16.1 ± 2.3 mm); a sharp PV atrium angle and excessively superior transseptal puncture might preclude cannulation.

ROOF LINE. In total, 8 patients had prior roof-line ablation. Only 1 patient had conduction block through the roof line and no CMR gaps. Of the 7 patients with conduction resumption at the time of the reablation procedure, 5 had CMR gaps at the roof line and 2 showed complete absence of scarring (Online Fig. 3). The most common location for the CMR gaps was the right aspect of the roof line (60%). Two patients had gaps at the left aspect or middle of the roof line. The mean length of the roof-line gaps was 21 ± 11 mm. The median RF time to achieve bidirectional block was 1.4 (IQR: 0.7 to 3.1) min.

ELECTROPHYSIOLOGICAL DATA AND DE-CMR CORRELATION. A very high-density voltage map was obtained in all patients, with a mean of 808 points (range 520 to 1,004). The median voltage (IQR) of the points located within scar, border zone, and healthy areas were 0.21 (0.10 to 0.36), 0.31 (0.17 to 0.51), and 0.44 (0.24 to 0.99) mV, respectively ($p < 0.001$). Gap identification was evaluated for both techniques in 10 patients: the mean number of identified gaps per patient was 7.2 ± 2.7 for DE-CMR and 5.5 ± 2.1 for high-density voltage map ($p = 0.016$), with agreement between both techniques of 76 ± 24% (Fig. 3).

DE-CMR–GUIDED PV REISOLATION. Of 46 reconnected PVs with CMR gaps, 44 (95.6%) were isolated only with the guidance of the DE-CMR model and 14 (30.4%) were isolated before completing the ablation of all gaps (Fig. 4, Online Video 1). Only 2 (4.4%) required the circular mapping catheter to identify the reconnection site. Complete circumferential lesions were deployed around the 3 PVs without identifiable scarring. The median RF time to achieve conduction block in all reconnected PVs was 13.3 (IQR: 7.5 to 21.7) min/patient (4.2 min/PV) (Table 3). Bidirectional block trough of the roof line was achieved after a median 1.4 min (IQR: 0.7 to 3.1) of RF (Fig. 5).

Compared with the 15 control procedures guided by a conventional circular mapping catheter, the DE-CMR approach significantly shortened mean RF time (1,441 ± 915 s vs. 930 ± 662 s; $p = 0.026$), but not the mean procedural duration (177 ± 50 min vs. 166 ± 65 min; $p = 0.633$) or median fluoroscopy time (18 [IQR: 11 to 27] min vs. 14 [10 to 18] min; $p = 0.343$), respectively.

DISCUSSION

MAIN FINDINGS. The present study showed that: 1) identification of atrial scarring and gaps by DE-CMR is

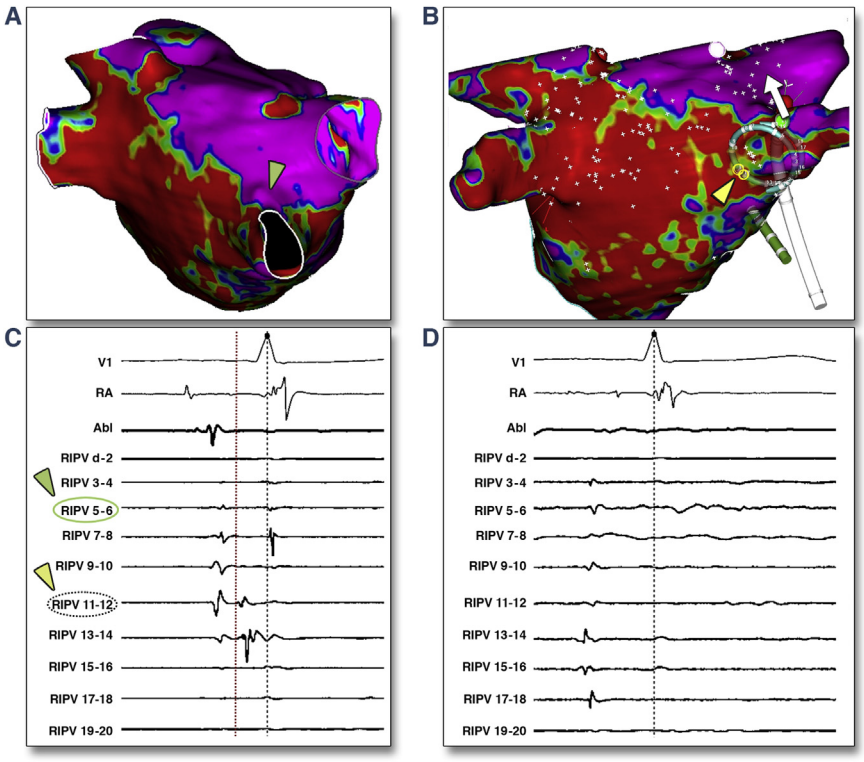

FIGURE 2 Example of No Concordance in the Assessment of the Reconnection Site by Circular Mapping Catheter and DE-CMR Model

(A) DE-CMR model showing a gap at the superior part of the right inferior pulmonary vein (RIPV) **(green arrowhead)**. **(B)** Ablation catheter at anatomic gap site. Lasso catheter positioned at RIPV shows **(C)** earliest activation at dipole 11 to 12 **(yellow arrowhead)** that corresponds to the inferoposterior part of RIPV. **(D)** Radiofrequency application at CMR gap (dipole 5 to 6) led to pulmonary vein isolation. This example highlights the Lasso catheter's limitations in locating the reconnection site and the usefulness of DE-CMR. Abbreviation as in Figure 1.

feasible and accurate (Online Fig. 4); 2) DE-CMR can successfully guide the ablation of both circumferential antral lesions and additional ablation lines; and 3) DE-CMR has the potential to reduce RF ablation requirements. Finally, the identification of nonconducting DE-CMR gaps warrants further research to determine whether these are electrically dormant gaps that could eventually reconnect.

CMR IMAGING VISUALIZATION OF PREVIOUS ABLATION LESIONS AND GAPS. Robust evidence supports PV reconnection as the major cause of AF recurrence (4,5,19). Breaks in prior PVI ablation lesions are proposed as an underlying mechanism for this phenomenon (6,7). However, intraprocedural assessment of complete encircling lesions remains based on electrical parameters of conduction block within the PV ostia, both in first and repeated procedures.

In 2007, Peters et al. (9) described the capability of DE-CMR to detect previous PVI ablation lesions in the LA. McGann et al. (10) reported not only the usefulness of DE-CMR to detect RF lesions but also a correlation between the degree of scarring and procedural outcomes, confirmed in other studies (20). Moreover, the researchers suggested a potential DE-CMR application to detect gaps (10). However, no studies have demonstrated the clinical applicability of this modality. It has been reported that a very low proportion of patients (7%) had complete encircling lesions around all PVs after 1 PVI procedure. Moreover, the presence of CMR gaps in all PVs was very common (11). In the present study, all patients had CMR gaps and electrical reconnection in at least 1 PV. In up to 73% of patients, all PVs were reconnected.

In previous animal models, the minimum spatial resolution of the 3-T scanner (1.25 × 1.25 × 2.5 mm) allowed the identification of gaps at the millimeter scale (13). In the present study, with the same spatial resolution, the minimum gap length was

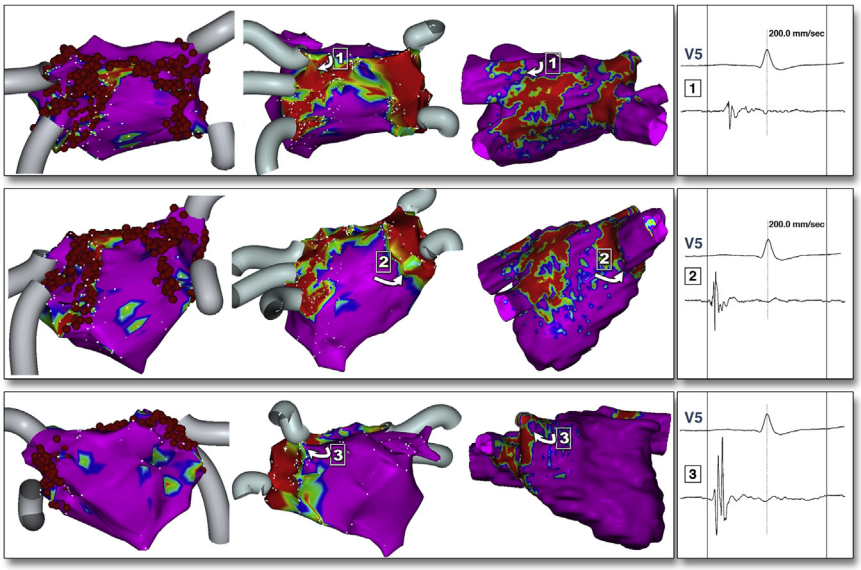

FIGURE 3 Comparison of Gap Definition Between High-Density Voltage Map and DE-CMR Model

Example of good scar correlation between voltage map and DE-CMR. Posterosuperior **(upper)**, posterolateral **(middle)**, and anteroseptal **(bottom)** views of the voltage map (ablation points shown as red dots; voltage thresholds: 0.3 to 0.6 mV) of the previous procedure **(left)**; the high-density voltage map of the repeated procedure **(middle)**; and the DE-CMR model **(right)**. White arrows indicate gap sites. Images show good agreement between the voltage map and DE-CMR model but better accuracy in gap definition with DE-CMR. Note the good agreement between the location of the ablation sites and the post-procedural scarring. Electrograms recorded at the CMR gaps are shown in the right panel. Abbreviation as in Figure 1.

1.6 mm. Remarkably, a very high rate of PV reisolation was achieved, targeting only the CMR gaps, which suggests that all conducting gaps could potentially be identified by DE-CMR. If this hypothesis is confirmed in a larger study, DE-CMR might be proposed as a reliable guide for reablation procedures.

CMR IMAGING AND VOLTAGE MAPPING. In the present study, we found that most of the electrical reconnection sites assessed by the Lasso catheter (79%) matched a CMR gap. The study by Spragg et al. (12) reported that DE-CMR had poor accuracy in localizing PV reconnection sites. They found that DE-CMR could identify the reconnection site in only 28% of PVs. The conflicting results might be partially explained by differences in scanner and coil features, image acquisition protocol, and post-processing tools, which may affect the signal-to-noise ratio and have an impact on image quality. Spragg et al. (12) used manual segmentation of the areas presenting visual hyperenhancement. Although the researchers validated this method for ventricular scar analysis, it might be inaccurate at the atrial level due to the thin atrial wall. We used a 3-T scanner with a 32-channel cardiac coil, which optimized the signal-to-noise ratio and improved image quality. Complete LA wall segmentation was performed to avoid operator-dependent assessment of scar boundaries. An automated protocol based on pixel intensity was applied to better define hyperenhanced areas and gaps. Additionally, the high PV reisolation rate in our study suggests that CMR is sufficiently accurate to localize the reconnection site, even in those cases when the earliest activation did not match a CMR gap (Fig. 4).

We compared the capability to detect anatomic gaps between DE-CMR and the electroanatomic map. We strived to optimize the electroanatomic mapping and improve the accuracy of the technique by overcoming its main limitations. We created a very high-density map (mean of 808 points) to reduce the interpolation, which decreased the spatial resolution and worsened the visualization of gaps. Using contact-force guidance avoided false low-voltage areas, which could potentially hide actual gaps. Despite these efforts, we found that DE-CMR identified higher numbers of gaps than voltage mapping (7.2 $\pm$ 2.7 gaps vs. 5.5 $\pm$ 2.1 gaps), suggesting that CMR might be

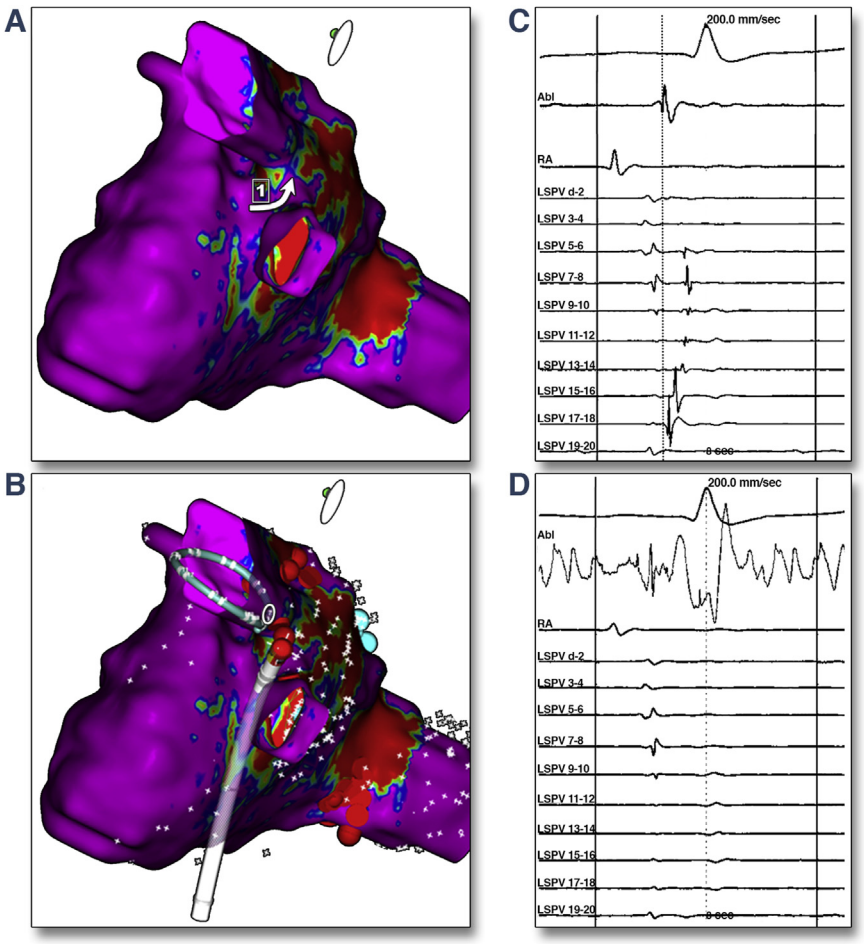

FIGURE 4 Example of a CMR Imaging-Guided Ablation of Gaps Leading to LSPV Reisolation

(A) Left atrial lateral projection of the DE-CMR model showing a gap at the carina **(white arrow)**. **(B)** Lasso catheter into left superior pulmonary vein (LSPV) and ablation catheter located in the gap (white circle shows D-2 Lasso dipole position). **(C)** ThermoCool SmartTouch and Lasso catheter (Biosense Webster) electrograms before ablation show PV potentials. The gap in DE-CMR correlates with D-2 Lasso dipole position **(white circle)**, showing earliest PV potential **(dotted line)**. **(D)** Lasso catheter electrograms after radiofrequency application. PV isolation was achieved after 68 s of application at the gap site. Also see accompanying Online Video 1. PV = pulmonary vein; other abbreviation as in Figure 1.

more accurate in defining the presence and location of anatomic gaps. Additionally, DE-CMR achieved better qualitative definition of the gaps than voltage mapping (Fig. 3).

CMR IMAGING GUIDANCE FOR ABLATION OF GAPS. Although previous reports have suggested a potential use of this imaging modality to identify ablation line gaps (14), and even to guide the ablation in acute ablation sets in animal models (13), the present study is, to the best of our knowledge, the first to apply direct DE-CMR guidance, integrating the DE-CMR model into the navigation system, to ablate gaps in humans. Using only the DE-CMR model to guide catheter positioning, gaps can be successfully targeted and PVI achieved. Bidirectional block was achieved in nearly 96% of PVs and in all of the roof lines. Additionally, the DE-CMR model identified those PVs without any degree of scarring, allowing the planning of the ablation approach (complete encirclement vs. ablation of gaps).

A substantial number of PVs were electrically but not anatomically isolated; up to 43% of the baseline

TABLE 3 Procedural Characteristics

Patient #	Total RF Time (min)	RF Time to PVI (min)	RF Time/ Gap (min)	Procedure Time (min)	Fluoroscopy Time (min)	Successful CMR-Guided Isolation	PV Lasso Cannulation Failure
All	18.6 ± 10.9	14.91 ± 9.19	3.5 ± 2.3	147.0 ± 56.8	14.1 ± 4.9	44/46	8/53
1	9.4	8.0	2.0	75	10	4/4	0/4
2	14.1	10.5	2.1	240	9	4/4	2/4
3	38.4	31.2	7.8	195	12	4/4	0/4
4	3.7	3.7	0.6	150	10	3/3	0/4
5	41.8	25.8	5.2	270	11	3/3	0/3
6	8.0	5.3	1.3	120	19	2/2	0/3
7	14.6	13.3	3.3	160	18	3/3	0/4
8	13.1	11.9	6.0	80	20	2/2	0/2
9	9.9	2.9	0.9	180	17	3/3	1/3
10	29.0	29.0	5.8	114	14	3/4	0/4
11	19.3	15.8	2.6	125	12	3/4	1/4
12	19.0	16.1	2.7	120	23	3/3	1/3
13	23.1	20.0	6.7	180	12	2/2	1/4
14	23.5	23.5	3.9	120	19	3/3	1/4
15	12.0	7.1	1.8	90	6	2/2	1/3

RF = radiofrequency; other abbreviations as in Tables 1 and 2.

isolated PVs showed CMR gaps, highlighting the potential role of dormant gaps as the mechanism for late recurrences (21). In such cases, DE-CMR might identify potential reconnection sites that are otherwise undetectable, and improve clinical outcome. However, further studies are needed to confirm this hypothesis.

CIRCULAR MULTIPOLAR CATHETER APPROACH. In 14.3% of PVs, cannulation of the circular catheter was not feasible due to narrowness, sharp angles, or location with respect to the transseptal access, hampering identification of the earliest activation site and the demonstration of bidirectional block. Reisolation in this scenario could lead to the creation of complete encircling lesions, increasing the RF delivery and procedural requirements. The DE-CMR approach helps to locate the gap and guides catheter positioning, potentially avoiding the need for a circular catheter. In this study, 96% of PVs were reisolated with the sole guidance of the DE-CMR model. Only 2 PVs (4.4%) required the use of a multipolar circular catheter to localize the gap; isolation was not achieved in 1 of these.

In the present study, a significant shortening of RF time was observed compared with a series of consecutive patients undergoing conventional PV reisolation. No differences in procedural time were found, probably because the acquisition of a very high-density map (for research purposes only) in the DE-CMR group could have overestimated the overall procedure duration; a much lower density is required to merge CMR images in clinical practice.

CLINICAL IMPLICATIONS. DE-CMR may help to plan repeated procedures by assessing the number, location, and length of gaps; facilitate the achievement of PVI, reduce RF ablation time, and potentially shorten procedural duration.

The study results also suggest that DE-CMR identification of gaps might be enough to guide the ablation procedure. Thus, a multipolar circular catheter might be needless in this setting, and only a single transseptal access would be required. Further studies are needed to confirm this hypothesis.

STUDY LIMITATIONS. The main study limitations are the small sample size and length of follow-up. The goal was to evaluate the usefulness of this approach in achieving acute PVI and therefore only short-term follow-up is reported. Conceived as a feasibility and "proof-of-concept" study, the present analysis does not compare conventional circular mapping catheter-guided ablation and the CMR-guided approach. In this study, we did not compare the benefit of ablating the CMR gaps until PVI was achieved with that of ablating all CMR gaps. Comparative studies are needed to evaluate the clinical impact of our new approach. Additionally, time between the first and index procedure varied widely. Although hyperenhancement characteristics and the reconnection mechanism might differ among patients, the study evaluated the DE-CMR model's capability to depict gaps at the time

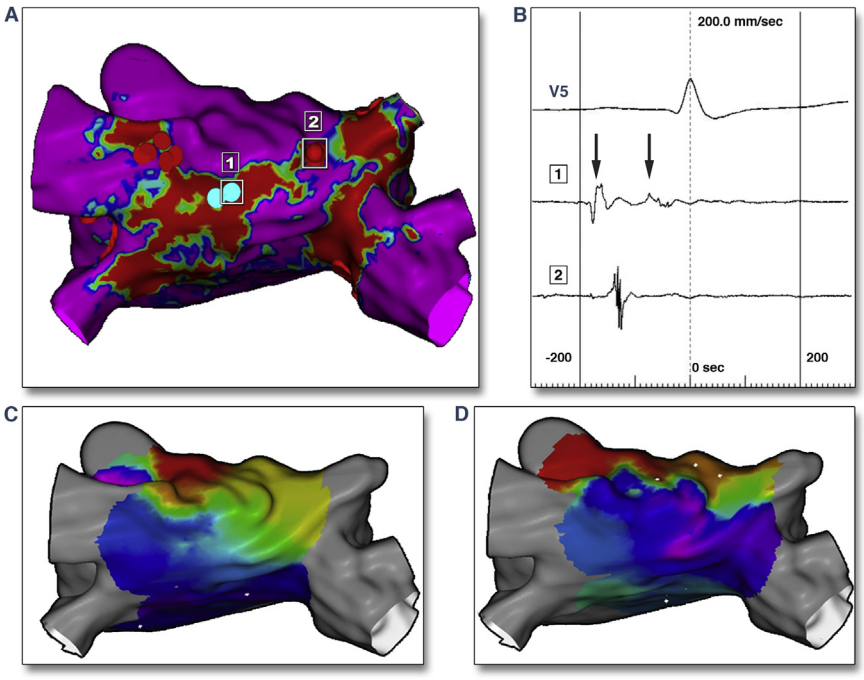

FIGURE 5 Example of a CMR-Guided Ablation of a Roof-Line Gap Leading to Bidirectional Conduction Block

(A) Roof-line scar **(red)**, shown in the superior view of the DE-CMR model. Blue dots correspond to electrograms with double potentials **(B-1)**. **Red dots** correspond to ablation site at the gap with normal electrogram **(B-2)**. Ablation at this point achieved linear block at roof line with a single application (62 s). **(C)** Activation map during left atrial appendage pacing before ablation, showing conduction through the roof line. **(D)** Activation map during left atrial appendage pacing after ablation, confirming complete block at roof line. Abbreviation as in Figure 1.

of the procedure, independently of the mechanism, and to test its usefulness in catheter ablation guidance. Although initial data have been reported (22), more comprehensive studies evaluating the long-term evolution of post-procedural atrial scarring are needed to clarify the behavior of the ablation lesions. Errors in the manual segmentation of the endocardium and epicardium of the LA could lead to the inclusion in the 3D model of extracardiac structures such as descending aorta or the blood pool. However, we carefully designed the image-processing methodology to address this potential issue. After the manual segmentation, we created 5 intermediate layers without thickness between the endocardium and epicardium and selected the layer that was entirely within the LA wall. This minimized the risk of picking up extracardiac structures. Currently there is no standard for the DE-CMR acquisition, image processing, and SI thresholds used to define healthy/scarred myocardium. In this study, the SI thresholds were based on previous studies by our group to characterize the ventricular myocardium (14,17). Further studies are needed to validate and standardize the cutoffs for the atrial myocardium.

CONCLUSIONS

DE-CMR can successfully guide PV reisolation procedures by accurately identifying and localizing the gaps. Moreover, DE-CMR may identify non-conducting gaps that could be related to later recurrences. This novel technique has the potential to facilitate the planning and execution of ablation procedures and reduce procedural duration and RF application time.

ACKNOWLEDGMENTS The authors thank Neus Portella for research assistance, Elaine Lilly for editorial assistance, and Mireia Calvo, MSc, for data collection.

REPRINT REQUESTS AND CORRESPONDENCE: Dr. Antonio Berruezo, Arrhythmia Section, Cardiology Department, Hospital Clinic, C/Villarroel 170, 08036 Barcelona, Spain. E-mail: berruezo@clinic.ub.es.

REFERENCES

1. Ouyang F, Tilz R, Chun J, et al. Long-term results of catheter ablation in paroxysmal atrial fibrillation: lessons from a 5-year follow-up. Circulation 2010;122:2368–77.

2. Weerasooriya R, Khairy P, Litalien J, et al. Catheter ablation for atrial fibrillation: are results maintained at 5 years of follow-up? J Am Coll Cardiol 2011;57:160–6.

3. Bisbal F, Guiu E, Calvo N, et al. Left atrial sphericity: a new method to assess atrial remodeling. Impact on the outcome of atrial fibrillation ablation. J Cardiovasc Electrophysiol 2013;24:752–9.

4. Verma A, Kilicaslan F, Pisano E, et al. Response of atrial fibrillation to pulmonary vein antrum isolation is directly related to resumption and delay of pulmonary vein conduction. Circulation 2005;112:627–35.

5. Ouyang F, Antz M, Ernst S, et al. Recovered pulmonary vein conduction as a dominant factor for recurrent atrial tachyarrhythmias after complete circular isolation of the pulmonary veins: lessons from double Lasso technique. Circulation 2005;111:127–35.

6. Kowalski M, Grimes MM, Perez FJ, et al. Histopathologic characterization of chronic radiofrequency ablation lesions for pulmonary vein isolation. J Am Coll Cardiol 2012;59:930–8.

7. Ranjan R, Kato R, Zviman MM, et al. Gaps in the ablation line as a potential cause of recovery from electrical isolation and their visualization using MRI. Circ Arrhythm Electrophysiol 2011;4:279–86.

8. Dickfeld T, Kato R, Zviman M, et al. Characterization of radiofrequency ablation lesions with gadolinium-enhanced cardiovascular magnetic resonance imaging. J Am Coll Cardiol 2006;47:370–8.

9. Peters DC, Wylie JV, Hauser TH, et al. Detection of pulmonary vein and left atrial scar after catheter ablation with three-dimensional navigator-gated delayed enhancement MR imaging: initial experience. Radiology 2007;243:690–5.

10. McGann CJ, Kholmovski EG, Oakes RS, et al. New magnetic resonance imaging-based method for defining the extent of left atrial wall injury after the ablation of atrial fibrillation. J Am Coll Cardiol 2008;52:1263–71.

11. Badger TJ, Daccarett M, Akoum NW, et al. Evaluation of left atrial lesions after initial and repeat atrial fibrillation ablation: lessons learned from delayed-enhancement MRI in repeat ablation procedures. Circ Arrhythm Electrophysiol 2010;3:249–59.

12. Spragg DD, Khurram I, Zimmerman SL, et al. Initial experience with magnetic resonance imaging of atrial scar and co-registration with electroanatomic voltage mapping during atrial fibrillation: success and limitations. Heart Rhythm 2012;9:2003–9.

13. Ranjan R, Kholmovski EG, Blauer J, et al. Identification and acute targeting of gaps in atrial ablation lesion sets using a real time MRI system. Circ Arrhythm Electrophysiol 2012;5:1130–5.

14. Fernández-Armenta J, Berruezo A, Andreu D, et al. Three-dimensional architecture of scar and conducting channels based on high resolution ce-CMR: insights for ventricular tachycardia ablation. Circ Arrhythm Electrophysiol 2013;6:528–37.

15. Larrabide I, Omedas P, Martelli Y, et al. Gimias: an open source framework for efficient development of research tools and clinical prototypes. Funct Imaging Model Heart 2009;5528:417–26.

16. GIMIAS. Available at: www.gimias.org. Accessed April 28, 2014.

17. Andreu D, Berruezo A, Ortiz-Perez JT, et al. Integration of 3D electroanatomic maps and magnetic resonance scar characterization into the navigation system to guide ventricular tachycardia ablation. Circ Arrhythm Electrophysiol 2011;4:674–83.

18. Tamborero D, Mont L, Berruezo A, et al. Circumferential pulmonary vein ablation: does use of a circular mapping catheter improve results? A prospective randomized study. Heart Rhythm 2010;7:612–8.

19. Cappato R, Negroni S, Pecora D, et al. Prospective assessment of late conduction recurrence across radiofrequency lesions producing electrical disconnection at the pulmonary vein ostium in patients with atrial fibrillation. Circulation 2003;108:1599–604.

20. Peters DC, Wylie JV, Hauser TH, et al. Recurrence of atrial fibrillation correlates with the extent of post-procedural late gadolinium enhancement: a pilot study. J Am Coll Cardiol Img 2009;2:308–16.

21. Arentz T, Macle L, Kalusche D, et al. "Dormant" pulmonary vein conduction revealed by adenosine after ostial radiofrequency catheter ablation. J Cardiovasc Electrophysiol 2004;15:1041–7.

22. Higuchi K, Akkaya M, Koopmann M, et al. Long-term radio-frequency scar behavior after ablation of atrial fibrillation: lessons learned from LGE-MRI. Circulation 2012;126:A18083.

KEY WORDS atrial fibrillation, catheter ablation, delayed-enhancement, gaps, magnetic resonance imaging

APPENDIX For a supplemental video and legend, methods, and figures, please see the online version of this article.